Speciation of Nanoscale Objects by Nanoparticle Imprinted Matrices

- Supporting Information -

Maria Hitrik[1], Yamit Pisman[1] and Gunther Wittstock[2]* and Daniel Mandler[1]*

[1] Institute of Chemistry, the Hebrew University of Jerusalem, Jerusalem 9190401, Israel

E-mail: daniel.mandler@mail.huji.ac.il

[2] Institute of Chemistry, Center of Interface Science, Faculty of Mathematics and Natural Sciences, Carl von Ossietzky University of Oldenburg, Oldenburg, D-26111, Germany

Content

S-1 Experimental

S-1.1 AuNP synthesis

Synthesis of AuNPs. Citrate stabilized spherical AuNPs (10 ± 2 nm and 40 ± 2 nm) were synthesized according to Bastus et al.[1] based on a kinetic control of the NP growth. After boiling 150 ml of 2.2 mol l^{-1} sodium citrate in water solution for 15 min, 1 ml of $HAuCl_4$ (25 mmol l^{-1}) was injected with vigorously stirring. The solution was continuously heated until the color changed from yellow to bluish gray and then within 10 min to deep purple. The solution was cooled to room temperature and diluted to 375 ml with deionizer water. This resulted in the formation of 10 nm diameter AuNPs. In order to obtain larger AuNPs of 40 nm diameter, the boiling purple solution was cooled to 90 °C. Then, 1 ml of $HAuCl_4$ (2.2 mmol l^{-1}) and 1 ml of citrate (60 mmol l^{-1}) were added every 30 min, up to 14 additions. It should be noted that according to Bastus et al. these additions caused only the existing particles growth and not the formation of new AuNPs. The particles were examined by extra high-resolution scanning electron microscopy (XHR-SEM). The final solution was diluted to 375 ml total.

S-1.2 AgNP synthesis

For the synthesis of citrate stabilized spherical AgNPs[2] 100 ml of aqueous solution containing 5 mmol l^{-1} trisodium citrate and 0.025 mmol l^{-1} tannic acid was prepared and heated to boiling in a three-neck round bottomed flask for 15 min under vigorous stirring. A condenser was used to prevent the evaporation of the solvent. After boiling, 1 ml of $AgNO_3$ (25 mmo l^{-1}) was injected into this solution. The color of the solution turned yellow. The resultant AgNPs were purified by centrifugation (10,000 g) in order to remove the excess of TA with further re-dispersion in deionized water before sample characterization. The obtained AgNPs had a diameter of (10 ± 3) nm.

S-1.3 Instrumentation

Electrochemical measurements were conducted with a CHI bipotentiostat (model 750, CH Instruments, Austin, TX). All the electrochemical measurements were performed at room temperature using a conventional three-electrode cell with Ag/AgCl/1 M KCl and Pt wire as reference and auxiliary electrodes, respectively. All potentials are given with respect to Ag/AgCl/1 M KCl. Water contact angles were collected with a Rame-Hart 100 goniometer (Rame-Hart Instrument Co., Succasunna, NJ, USA) equipped with automated dispensing system, with 2.5 µl water drops.

Extra high-resolution scanning electron microscopy (XHR-SEM) was carried out with a Magellan 400L (FEI, USA) without any pretreatment of the ITO samples. The particles density was calculated using Image-J software. Atomic force microscopy (AFM) of ITO samples was performed with a NanoScope IVa controller attached to a Dimension 3100 instrument (Veeco Digital Instruments, Santa Barbara, CA) in the tapping mode using Si tips (SCD15-AlBS, Mikromasch, Estonia). A NanoScope IIIa controller (Digital Instruments Veeco Metrology Group) was used for imaging the Si substrates.

[1] Bastus, N. G.;Comenge, J.; Puntes, V. Kinetically Controlled Seeded Growth Synthesis of Citrate-Stabilized Gold Nanoparticles of up to 200 nm: Size Focusing versus Ostwald Ripening. *Langmuir* **2011**, *27*, 11098-11105.

[2] Bastus, N. G.;Merkoci, F.;Piella, J.; Puntes, V. Synthesis of Highly Monodisperse Citrate-Stabilized Silver Nanoparticles of up to 200 nm: Kinetic Control and Catalytic Properties. *Chem. Mater.* **2014**, *26*, 2836-2846.

S-2 Immobilization of AuNPs on ITO and ITO treated by PEI

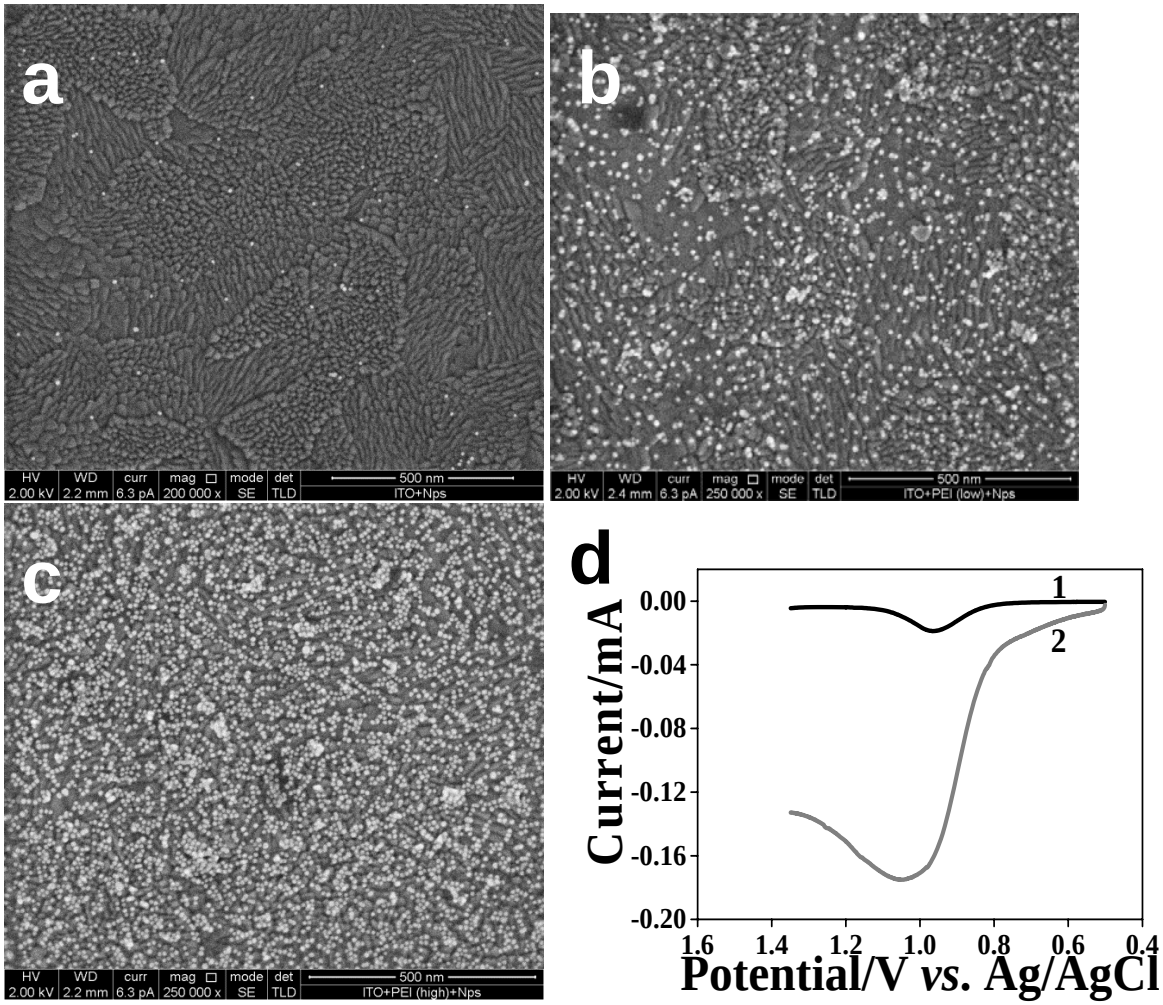

Figure S-2. SEM images of ITO after adsorption of AuNPs (1 h): (a) ITO, (b) ITO/PEI/AuNPs with PEI 0.72 mg ml^{-1}, (c) – ITO/PEI/AuNPs with PEI 3 mg ml^{-1}, (d) LSV obtained with ITO electrode after adsorption of: curve 1 – ITO/AuNPs, curve 2 – ITO/(PEI 0.72 mg ml^{-1})/AuNPs (1 h). The electrolyte solution contained 0.1 KCl and scan rate was 0.05 V s^{-1}.

These SEM images together with LSV results demonstrated a clear correlation between the density of AuNPs adsorbed on ITO and the preceding adsorption of PEI layer. The prior treatment with PEI improved the adsorption of AuNPs and gave more reproducible results. In addition, the PEI bath concentration affected the AuNPs adsorption, i.e. increasing the concentration of the PEI in the solution, yielded more adsorbed particles.

S-3 Time dependence of immobilization of AuNPs on ITO treated by PEI

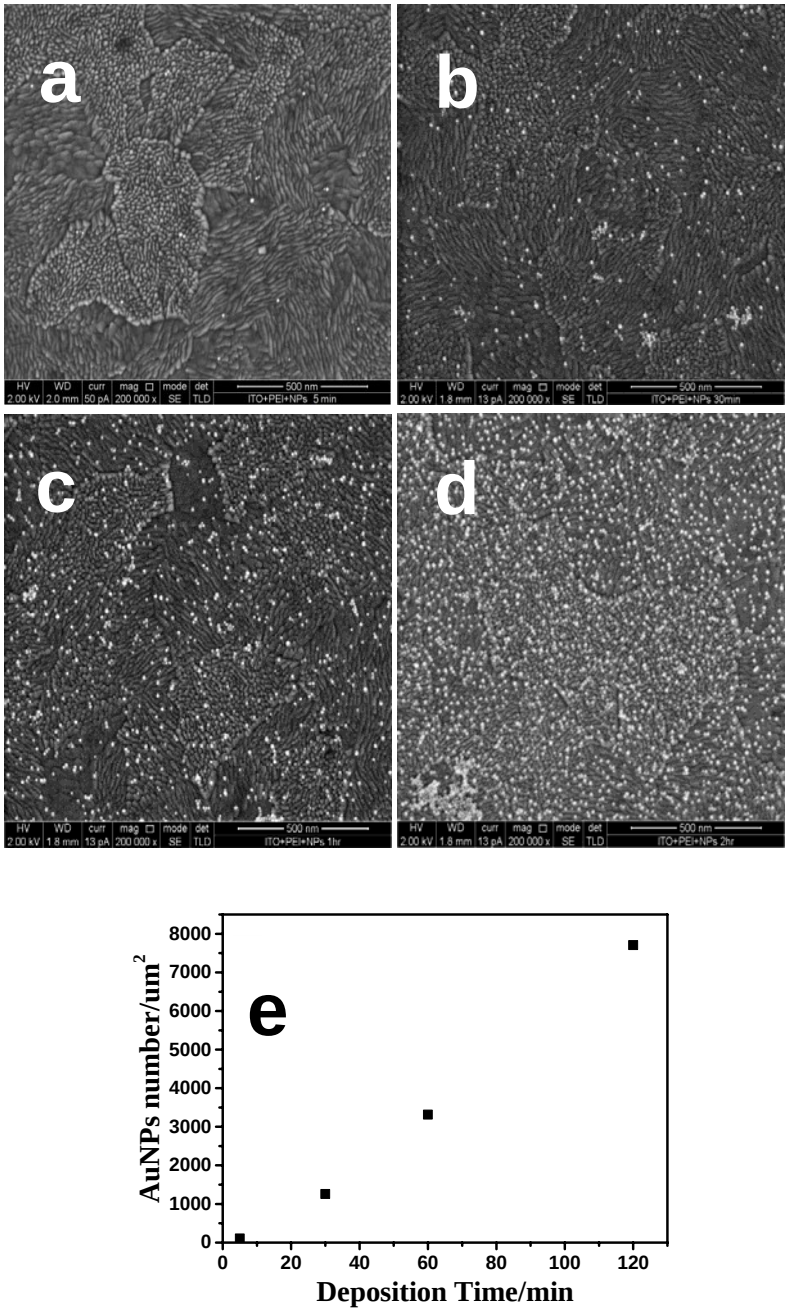

Figure S-3. SEM images of ITO surfaces treated first by 0.72 mg ml^{-1} PEI for 2 h followed by adsorption from AuNPs solution for (a) 5 min, (b) 30 min, (c) 60 min and (d) 120 min., (e) AuNPs surface density as a function of AuNPs deposition time.

S-4 CV obtained with ITO/PEI/OA and ITO/PEI/PAA

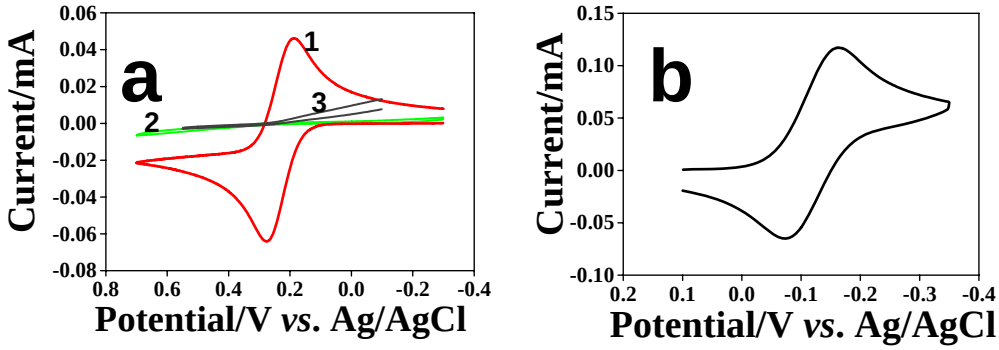

Figure S-4. (a) - CV recorded in 1 mM $[Fe(CN)_6]^{4-}$ and 0.1 M KCl with (1) ITO/PEI (2) ITO/PEI/OA and (3) ITO/PEI/PAA; (b) CV of 1 mM $[Ru(NH_3)_6]^{3+}$ in 0.1 M KCl with ITO/PEI/PAA. Scan rate 0.05 V s^{-1}.

From these CVs, it is evident that the OA and PAA cover the non-occupied areas very well and allow charge transfer through the AuNPs only embedded in ITO/PEI/AuNPs/OA or ITO/PEI/AuNPs/PAA. At the same time, the non-occupied areas that were filled with PAA do not block electron transfer by electroactive species that are not negatively charged.

S-5 LSV obtained with ITO/PEI/AuNPs/PAA

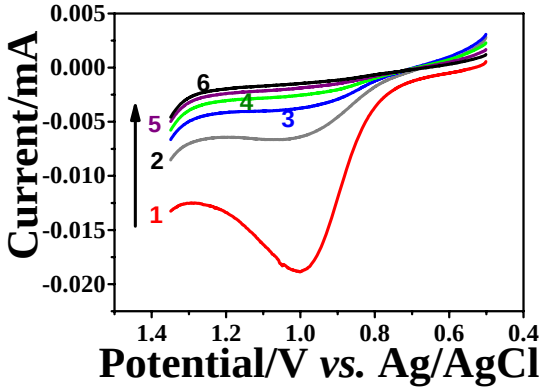

Figure S-5. Electrooxidation of AuNPs. Successive LSV of ITO/PEI/AuNPs/PAA recorded in 0.1 M KCl with 0.05 V s^{-1}.

A clear oxidation wave at 1 V is seen in the first scan that is associated with the oxidative dissolution of the AuNPs to form $[AuCl_4]^-$. The peak area and peak height decreased in subsequent scans indicative for the removal of the AuNPs, which were almost completely removed after five scans.

S-6 Comparison of LSV peak potentials for the oxidation of AuNPs of different size

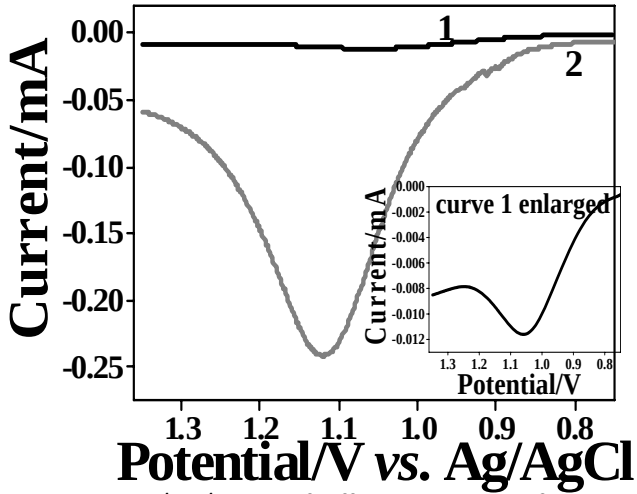

Figure S-6. LSV obtained with ITO/PEI/AuNPs of different diameters for 1 h: 1 – 10 nm, and 2 – 40 nm in 0.1 M KCl at a scan rate of 0.05 V s^{-1}.

The LSV curves 1 and 2 show the oxidation current of 10 and 40 nm particles, respectively. A clear shift to more positive potentials was obtained upon oxidation of larger AuNPs.

S-7 Schematic description of NAIM conductive area changes at different stages

Scheme S-1. A geometrical explanation of the change in the electroactive area of the ITO/PEI/AuNPs/PAA or ITO/PEI/AuNPs/OA before and after electrooxidation of the AuNPs. The arrow represents the electroactive surface (only one AuNP and one void were marked in each panel).

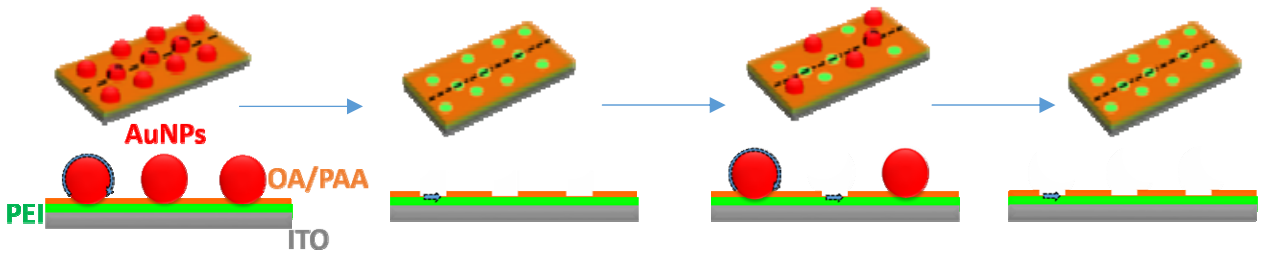

In the presence of imprinted AuNPs, charge transfer occurred through the nearly spherical NPs that were exposed to the electrolyte solution. However, once the AuNPs were removed, electron transfer took place in the voids at the ITO covered PEI surface.

S-8 CV obtained with ITO/PEI/10 nm AuNPs/OA or ITO/PEI/ 40 nm AuNPs/OA before and after AuNPs electrooxidation

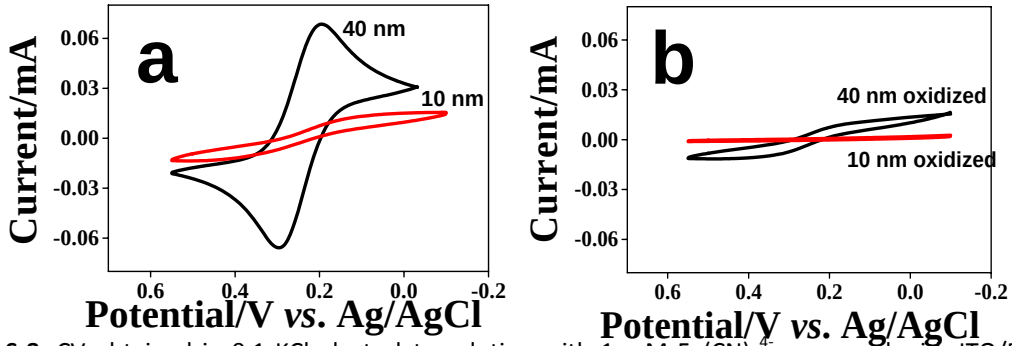

Figure S-8. CV obtained in 0.1 KCl electrolyte solution with 1 mM $Fe(CN)_6^{4-}$ measured with ITO/PEI/(40 nm AuNPs)/OA and ITO/PEI/(10 nm AuNPs)/OA assemblies: (a) before and (b) after oxidation.

NAIMs that were prepared according to the same protocol as for the 10 nm diameter AuNPs, but with the adsorption of 40 nm diameter NPs for 1 h. The surface became less conductive as a result of AuNPs removal. We found that 40 nm diameter AuNPs gave higher faradaic currents both, before (Figure S-7 (a)) and after (Figure S-7 (b)) AuNPs electrooxidation as compared with AuNPs of 10 nm diameter. Moreover, the CV obtained with the 40 nm AuNPs clearly indicates that the diffusion layers overlap in contrast with the CV of the 10 nm AuNPs, which exhibits a sigmoidal shape and is a consequence of separated hemispherical diffusion layers. These results clearly show that imprinting by AuNPs of 40 nm diameter (as compared to AuNPs of 10 nm diameter) increases the currents before and after oxidation due to overlapping of the diffusion layers of the electrode areas and increasing the exposed areas of the electrodes in the voids.

S-9 Calculation of number of adsorbed and reuptaken nanoparticles

The charge (*Q*) associated with oxidation or reduction wave obtained by linear sweep voltammetry with a scan rate *v*, can be calculated (Equation S1) by integrating the current *I* over the potential *E* after subtraction of the charging current.

$$Q = \frac{1}{v}\int I(E)dE \tag{1}$$

At the same time, the total charge obtained from oxidation of adsorbed AuNPs is given by:

$$Q = nq \tag{2}$$

Where *n* is a number of particles and *q* is an average charge per single AuNP. The number of Au atoms (*N*) in one AuNP is given by Equation S3, where *e* is the elemental charge.

$$N = \frac{q}{3e} \tag{3}$$

Obviously, larger NPs comprise larger number of Au atoms and therefore generate larger charge upon oxidation:

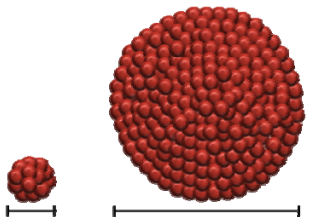

Scheme S-2 Size comparison of 10 and 40 nm particles, assuming identical density.

A nanoparticle with radius *r*, will give charge *q* upon oxidation (Equation S4):

$$q = \frac{4\pi r^3 dF}{mw} \tag{4}$$

Where *mw* and *d* are the atomic weight and density of gold, respectively, and *F* is the Faraday constant. Therefore, the ratio between the faradaic charges (or between the number of NPs, *n*) due to electrochemical oxidation of AuNPs depends on the cubic ratio between the radii of the nanoparticles (Equation S5):

$$\frac{q_{big}}{q_{small}} = \left(\frac{r_{big}}{r_{small}} \right)^3 \tag{5}$$

In order to compare the number of large and small AuNPs adsorbed onto the surface, the charges generated by larger AuNPs should be multiplied by the cubic ratio between the radii of the smaller to bigger nanoparticles (from Equation S2 and Equation S5):

$$\frac{n_{big}}{n_{small}} = \frac{Q_{big} q_{small}}{Q_{small} q_{big}} = \frac{Q_{big}}{Q_{small}} \left(\frac{r_{big}}{r_{small}} \right)^3 \tag{6}$$

S-10 Blank experiment: LSV obtained with non-imprinted ITO/PEI/OA and ITO/PEI/PAA after AuNPs adsorption

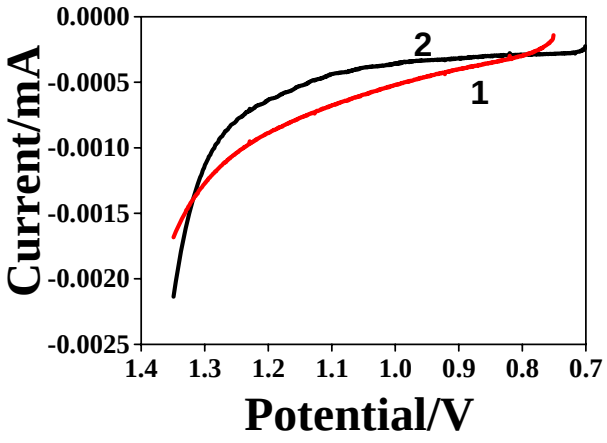

Figure S-10. LSV recorded in 0.1 M KCl with (1) ITO/PEI/OA and (2) ITO/PEI/PAA after adsorption of AuNPs for 1 h. Scan rate 0.05 V s^{-1}.

From the obtained electrooxidation waves, it can be concluded that no AuNPs were electrochemically detected at the ITO/PEI/PAA or ITO/PEI/OA assemblies upon immersion of these surfaces into the 10 nm AuNPs solution for 1 h.

S-11 SEM images of the blank experiment: adsorption of AuNPs onto ITO/PEI/OA and ITO/PEI/PA

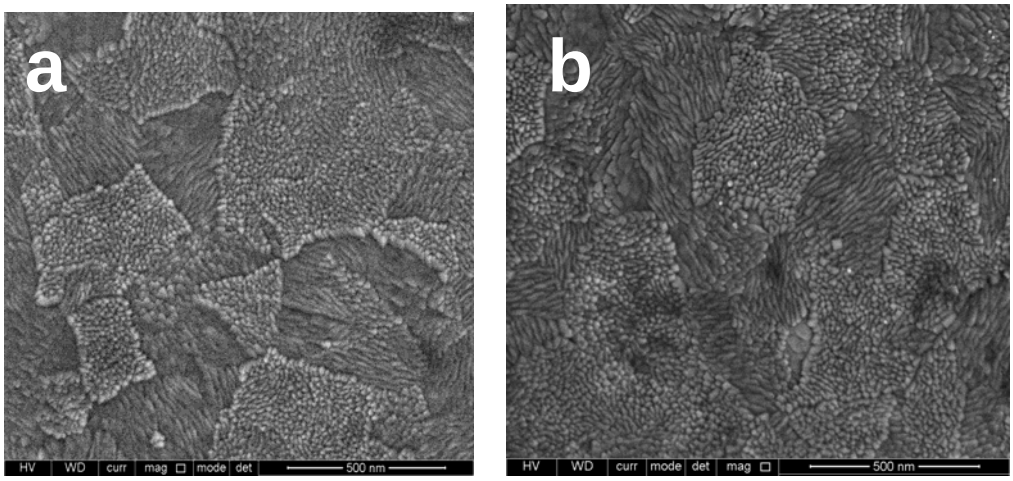

Figure S-11. SEM images of ITO/PEI/OA (a) or ITO/PEI/PAA (b) layers after immersion into a solution of 10 nm AuNPs for 1 h.

These blank experiments clearly show that non-imprinted ITO/PEI/OA and ITO/PEI/PAA layers are incapable of retaining AuNPs.

S-12 SEM images of reuptake of 10 nm diameter and 40 nm diameter AuNPs onto oxidized ITO/PEI/10 nm AuNPs/PAA

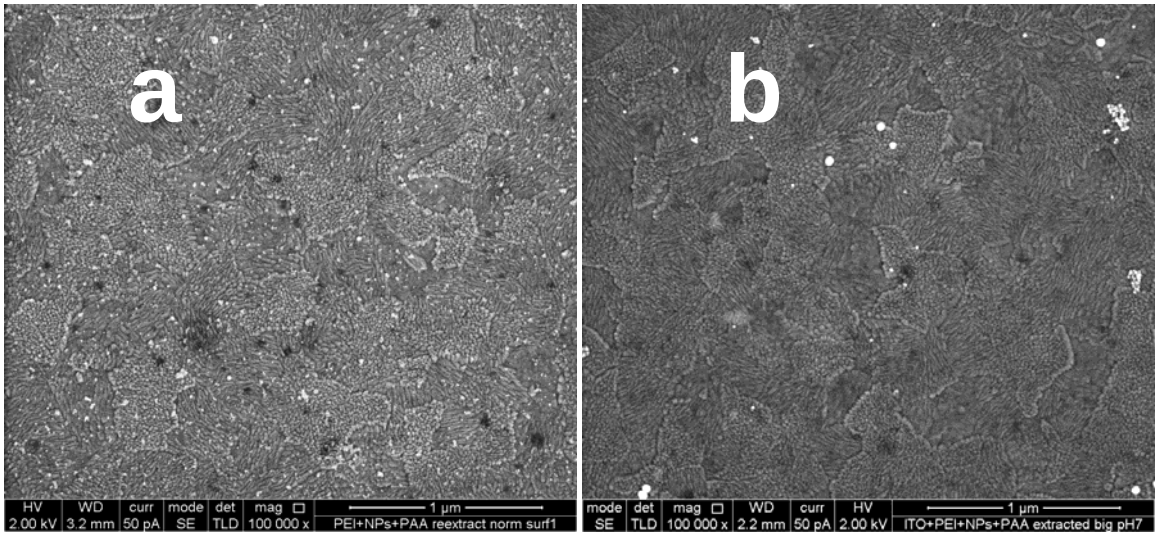

Figure S-12. Morphology images of ITO/PEI/SEM images of ITO/PEI/PAA imprinted by 10 nm AuNPs, after reuptake of AuNPs with 10 nm (a) and 40 nm (b) diameters.

Only a few 40 nm AuNPs were observed as a result of 10 nm particles reuptake by the ITO/PEI/PAA template imprinted with 10 nm particles.

S-13 Effect of thickening the matrix.

Scheme S-3. Schematic presentation of the selectivity increased associated with a thicker NAIM.